 CMC, vol.21, no.1, pp.1-15, 2011

Computation of Dyadic Green's Functions for Electrodynamics in Quasi-Static Approximation with Tensor Conductivity

V.G.Yakhno[1]

Abstract: Homogeneous non-dispersive anisotropic materials, characterized by a positive constant permeability and a symmetric positive definite conductivity tensor, are considered in the paper. In these anisotropic materials, the electric and magnetic dyadic Green's functions are defined as electric and magnetic fields arising from impulsive current dipoles and satisfying the time-dependent Maxwell's equations in quasi-static approximation. A new method of deriving these dyadic Green's functions is suggested in the paper. This method consists of several steps: equations for electric and magnetic dyadic Green's functions are written in terms of the Fourier modes; explicit formulae for the Fourier modes of dyadic Green's functions are derived using the matrix transformations and solutions of some ordinary differential equations depending on the Fourier parameters; the inverse Fourier transform is applied to obtained formulae to find explicit formulae for dyadic Green's functions.

Keywords: time-dependent Maxwell's equations, anisotropic conductivity tensor, dyadic Green's functions, analytical method, matrix transformations, simulation

1 Introduction

The presence of electrically anisotropic earth materials (brine, water, oil and gas) and biological tissues (white and gray matter, outer skull and skin) can have a profound effect on the interpretation of electromagnetic data. Modelling electromagnetic wave phenomena using $3D$ solution of Maxwell's equations with an anisotropic conductivity tensor and a constant magnetic permeability is used in a realistic head model and models of geophysics (see, for example, [Wang and Fang (2001)]; [Weiss and Newmann (2002)]; [Weiss and Newmann (2003)]; [Sekino and Yamaguchi (2003)]; [Darvas; Pantazis and Kucukaltun-Yildirim (2004)] ;

[1] Electrical and Electronics Engineering Department, DEU, Izmir, TURKEY.

[Young; Chen and Wong (2005)]; [Neuman and Alumbaugh (2002)]; [Commer et al. (2008)]). The dyadic Green's functions for electrically and magnetically isotropic materials have been widely used in different problems of electromagnetic wave theory (see, for example, [Tai (1994)]; [Kong (1986)]; [Lindell; Sihvola; Tretyakov; Vitanen (2002)]). Green's functions for equations of mathematical physics can be considered as a useful tool for different methods in the presentation of acoustic, electromagnetic, elastic and other fields, in particular, for the method of moments and boundary element method [Tai (1994)]; [Kong (1986)]; [Lindell; Sihvola; Tretyakov; Vitanen (2002)]; [Chew (1990)]; [Tewary (1995)]; [Tewary (2004)]; [Ting (2000)]; [Rashed (2004)]; [Ting (2005)]; [Nakamura and Tanuma (1997)]; [Pan and Yuan (2000)]; [Yang and Tewary (2008)]; [Gu; Young and Fan (2009)]; [Chen; Ke and Fan (2009)]. When the dyadic Green's functions can be constructed it leads to the significant simplification of modelling electromagnetic waves and allows engineers to overcome calculational difficulties [Tewary; Bartolo and Powell (2002)].

Dyadic Green's functions of the quasi-static Maxwell's equations are related to a singular impulsive electric current dipole source. The field due to a current dipole is considered in order to find an integral kernel that transforms a time-dependent distributed electric source $\mathbf{J}_p(x,t)$ into the electric field. In eddy-current problems, the unbounded domain dyadic kernel for a uniform isotropic conductor can be expressed in terms of a scalar Green's function satisfying the diffusion equation (see, for example, [Bowler (1999)]). The quasi-static dyadic Green's function for transient fields in a homogeneous conductive isotropic half-space has been derived by [Bowler (1999)] using the inverse Laplace transform by transforming the frequency domain expression to the time domain. In [Bowler and Fu (2006)] the time-dependent dyadic kernel has been constructed for an isotropic conductive plate from electric and magnetic scalar potentials and the inverse Laplace transform from the frequency domain to the time domain.

In the present paper we suggest a new method to derive the time-dependent dyadic Green's functions for quasi-static Maxwell's equations in conductive anisotropic media. This method consists of several steps: applying the Fourier transform with respect to the space variables, equations for electric and magnetic dyadic Green's functions are written in the terms of the Fourier images; explicit formulae for the Fourier images of dyadic Green's functions are derived using the matrix transformations and solving some ordinary differential equations depending on the Fourier parameters; the inverse Fourier transform is applied to obtained formulae to find explicit formulae for dyadic Green's functions. We note that the similar approach for constructing Green's functions and modelling and simulation electromagnetic fields in homogeneous anisotropic dielectrics has been successfully applied in the works [Yakhno (2005)], [Yakhno (2007)].

Generally, electromagnetic fields propagate with finite velocity. Electromagnetic fields in quasi-static approximation are time-dependent fields with negligible propagation effects [Dirks (1996)]. In applications where the wavelength of the studied electromagnetic fields is large compared to the extension of the studied object the wave propagation phenomena may be neglected. These 'slow-varying' fields are called as electromagnetic fields in quasi-static approximation. Looking into standard text books (see, for example, [Vagner; Lembrikov and Wyder (2004)]) we find that for the quasi-static approximation the displacement current density has to be neglected in Maxwell's first equation. Therefore the governing equations for the distribution of the electric and magnetic fields $\mathbf{E} = (E_1, E_2, E_3)$ and $\mathbf{H} = (H_1, H_2, H_3)$ throughout conductive anisotropic media are described by the time-dependent Maxwell's equations in the quasi-static approximation (see, for example, [Vagner; Lembrikov and Wyder (2004)]):

$$curl_x \mathbf{H} = \sigma_0 \bar{\bar{\sigma}} \mathbf{E} + \mathbf{J}_p, \quad (1)$$

$$curl_x \mathbf{E} = -\mu_0 \frac{\partial \mathbf{H}}{\partial t}, \quad (2)$$

$$div_x(\mathbf{H}) = 0. \quad (3)$$

where $x = (x_1, x_2, x_3)$ is a space variable from R^3, t is a time variable from R, $\mathbf{E} = (E_1, E_2, E_3)$, $\mathbf{H} = (H_1, H_2, H_3)$ are electric and magnetic fields, $E_k = E_k(x,t)$, $H_k = H_k(x,t)$, $k = 1,2,3$; $\mathbf{J}_p = (j_1, j_2, j_3)$ is the density of source currents responsible for the generation of eddy currents throughout a medium characterized by the electric conductivity tensor $\sigma = \sigma_0 \bar{\bar{\sigma}}$ and the magnetic permeability $\mu = \mu_0 \bar{\bar{I}}$, where σ_0, μ_0 are positive constants, $\bar{\bar{\sigma}} = (\sigma_{ik})_{3\times 3}$ is a symmetric positive definite 3×3 matrix and $\bar{\bar{I}}$ is the identity 3×3 matrix.

Equation (1) implies that

$$div_x(\sigma_0 \bar{\bar{\sigma}} \mathbf{E}) + div_x \mathbf{J}_p = 0.$$

In this paper we suppose that

$$\mathbf{E} = 0, \quad \mathbf{H} = 0, \quad \mathbf{J}_p = 0, \quad \text{for} \quad t < 0. \quad (4)$$

We note that equality (2) under condition (4) implies (3). We note also that equalities (1), (2) under condition (4) can be written in the form

$$\mu_0 \sigma_0 \bar{\bar{\sigma}} \frac{\partial \mathbf{E}}{\partial t} + curl_x curl_x \mathbf{E} = -\mu_0 \frac{\partial \mathbf{J}_p}{\partial t}, \quad \mathbf{E}|_{t<0} = 0, \quad (5)$$

$$\mu_0 \frac{\partial \mathbf{H}}{\partial t} = -curl_x \mathbf{E}, \quad \mathbf{H}|_{t<0} = 0. \quad (6)$$

The paper is organized as follows. Equations for electric and magnetic dyadic Green's functions of the time-dependent Maxwell's equations in the quasi-static approximation in a conductive anisotropic medium are written in Section 2. An explicit formula for k-th column of the electric dyadic Green's matrix is obtained in Section 3. Deriving an explicit formula for k-th column of the magnetic dyadic Green's matrix is given in Section 4. Section 5 describes the computational example and contains images of elements of electric and magnetic dyadic Green's matrices in a conductive anisotropic medium.

2 Equations for Dyadic Green's Functions

Let us consider a homogeneous conductive space with the conductivity $\sigma = \sigma_0 \bar{\bar{\sigma}}$ and the permeability $\mu = \mu_0 \bar{\bar{I}}$ satisfying above mentioned conditions. In the quasi-static regime for the considered homogeneous anisotropic medium, the electric dyadic Green's function $\mathscr{G}^E$ and the magnetic dyadic Green's function $\mathscr{G}^H$ are defined as electric and magnetic fields arising from impulsive current dipoles at $x = x^0$, $t = t^0$ and satisfying Maxwell's equations written as

$$curl_x \mathscr{G}^H(x - x^0, t - t^0) = \sigma_0 \bar{\bar{\sigma}} \mathscr{G}^E(x - x^0, t - t^0) + \bar{\bar{I}} \delta(x - x^0)\delta(t - t^0), \tag{7}$$

$$curl_x \mathscr{G}^E(x - x^0, t - t^0) = -\mu_0 \frac{\partial \mathscr{G}^H(x - x^0, t - t^0)}{\partial t}, \tag{8}$$

and vanishing for $t - t^0 < 0$ as well as $|x| \to \infty$ for all t. Here $x = (x_1, x_2, x_3)$ is 3-D space variable, $x^0 = (x_1^0, x_2^0, x_3^0)$ is 3-D parameter, t is the time variable, t^0 is the time parameter; $\bar{\bar{I}}$ is the unit tensor (the identity matrix of the order 3×3); $\delta(x - x^0) = \delta(x_1 - x_1^0)\delta(x_2 - x_2^0)\delta(x_3 - x_3^0)$, $\delta(x_j - x_j^0)$ is the Dirac delta function considered at $x_j = x_j^0$, $j = 1, 2, 3$; $\delta(t - t^0)$ is the Dirac delta function considered at $t = t^0$.

We note that $\mathscr{G}^E(x,t)$ and $\mathscr{G}^H(x,t)$ are matrices of 3×3 order. Let $\mathbf{E}^k(x,t) = (E_1^k(x,t), E_2^k(x,t), E_3^k(x,t))^T$ be the kth column of the matrix $\mathscr{G}^E(x,t)$ and $\mathbf{H}^k(x,t) = (H_1^k(x,t), H_2^k(x,t), H_3^k(x,t))^T$ be the kth column of the matrix $\mathscr{G}^H(x,t)$ then (7)-(8) can be written in terms of $\mathbf{E}^k(x,t)$ and $\mathbf{H}^k(x,t)$ for $x = (x_1, x_2, x_3) \in R^3$, $t \in R$ as follows

$$curl_x \mathbf{H}^k(x,t) = \sigma_0 \bar{\bar{\sigma}} \mathbf{E}^k(x,t) + \mathbf{e}^k \delta(x)\delta(t),$$

$$curl_x \mathbf{E}^k(x,t) = -\mu_0 \frac{\partial \mathbf{H}^k(x,t)}{\partial t}$$

with the following conditions

$$\mathbf{E}^k\big|_{t<0} = 0, \quad \mathbf{H}^k\big|_{t<0} = 0,$$

where $\mathbf{e}^1 = (1,0,0)^T$, $\mathbf{e}^2 = (0,1,0)^T$, $\mathbf{e}^3 = (0,0,1)^T$; the upper index T means the transpose of the row vectors to the column vectors.

Similar to introduction (determining (5), (6) from (1), (2)) we find that $\mathbf{E}^k(x,t)$ satisfies

$$\mu_0\sigma_0\bar{\bar{\sigma}}\frac{\partial \mathbf{E}^k}{\partial t} \quad + \quad curl_x curl_x \mathbf{E}^k = -\mu_0 \mathbf{e}^k \delta(x)\delta'(t), \quad \mathbf{E}^k\big|_{t<0} = 0, \tag{9}$$

and $\mathbf{H}^k(x,t)$ is defined by

$$\mu_0\frac{\partial \mathbf{H}^k}{\partial t} = -curl_x \mathbf{E}^k, \quad \mathbf{H}^k\big|_{t<0} = 0. \tag{10}$$

We note that the problem of determining the time-dependent electric and magnetic dyadic Green's functions is reduced to deriving solutions $\mathbf{E}^k(x,t)$ $(k=1,2,3)$ of (9). If $\mathbf{E}^k(x,t)$ $(k=1,2,3)$ are found then $\mathbf{H}^k(x,t)$ $(k=1,2,3)$ are derived as solutions of the initial value problems (10).

3 Deriving the Electric Dyadic Green's Function

The construction of a solution of (9) consists of several steps.

Step 1: Writing (9) in terms of the Fourier images with respect to $x = (x_1,x_2,x_3) \in R^3$. Let $\tilde{\mathbf{E}}^k(\nu,t)$ be the Fourier transform image of the electric field $\mathbf{E}^k(x,t)$ with respect to $x = (x_1,x_2,x_3) \in R^3$, i.e. the components of the Fourier mode of the electric field $\tilde{\mathbf{E}}^k(\nu,t) = (\tilde{E}_1^k(\nu,t),\tilde{E}_2^k(\nu,t),\tilde{E}_3^k(\nu,t))$ are defined by $\tilde{E}_j{}^k(\nu,t) = \mathscr{F}_x[E_j^k](\nu,t)$, $j=1,2,3$, where the Fourier operator $\mathscr{F}_x$ is given by (see, for example, [Vladimirov (1971)])

$$\mathscr{F}_x[E_j^k](\nu,t) = \int_{-\infty}^{+\infty}\int_{-\infty}^{+\infty}\int_{-\infty}^{+\infty} E_j^k(x,t)e^{i\nu\cdot x}dx_1dx_2dx_3,$$

$$\nu = (\nu_1,\nu_2,\nu_3) \in R^3; \quad \nu\cdot x = x_1\nu_1 + x_2\nu_2 + x_3\nu_3, \quad i^2 = -1.$$

Equations (9) can be written in the form of their Fourier images as follows

$$\mu_0\bar{\bar{\sigma}}\frac{\partial \tilde{\mathbf{E}}^k}{\partial t} + \mathscr{A}(\nu)\tilde{\mathbf{E}}^k = -\mu_0\mathbf{e}^k\delta'(t), \quad \tilde{\mathbf{E}}^k\Big|_{t<0} = 0, \tag{11}$$

where $\mathscr{A}(\nu)$ is the matrix defined by

$$\mathscr{A}(\nu)\tilde{\mathbf{E}}^k(\nu,t) \quad = \quad \mathscr{F}_x[curl_x curl_x \mathbf{E}^k(x,t)](\nu,t). \tag{12}$$

Using properties of the Fourier transform we find that $\mathscr{A}(\nu)$ is the symmetric positive semi-definite matrix whose elements are defined by

$$A_{11} = \nu_2^2 + \nu_3^2, \qquad A_{22} = \nu_1^2 + \nu_3^2, \qquad A_{33} = \nu_1^2 + \nu_2^2,$$
$$A_{12} = A_{21} = -\nu_1\nu_2, \quad A_{13} = A_{31} = -\nu_1\nu_3, \quad A_{23} = A_{32} = -\nu_2\nu_3.$$

Step 2: Reduction $\bar{\bar{\sigma}}$ and $\mathscr{A}(\nu)$ to diagonal form. The matrix $\bar{\bar{\sigma}}$ is symmetric positive definite and $\mathscr{A}(\nu)$ is symmetric positive semi-definite. In this step we construct a non-singular matrix $\bar{\bar{T}}$ and a diagonal matrix $\bar{\bar{D}}(\nu) = diag(d_1(\nu), d_2(\nu), d_3(\nu),)$ with non-negative elements such that

$$\bar{\bar{T}}^T(\nu)\bar{\bar{\sigma}}\bar{\bar{T}}(\nu) \;=\; \bar{\bar{I}}, \qquad \bar{\bar{T}}^T(\nu)\mathscr{A}(\nu)\bar{\bar{T}}(\nu) = \bar{\bar{D}}(\nu), \tag{13}$$

where $\bar{\bar{I}}$ is the identity matrix, $\bar{\bar{T}}^T(\nu)$ is the transposed matrix to $\bar{\bar{T}}(\nu)$. The similar reduction of pair symmetric matrices to diagonal form by congruence has been considered before by [Hong; Horn and Johnson (1986)] and [Goldberg (1992)]. Computing $\bar{\bar{D}}(\nu)$ and $\bar{\bar{T}}(\nu)$ can be made explicitly by the following way: firstly we find $\bar{\bar{\sigma}}^{-1/2}$ and then using the matrix $\bar{\bar{\sigma}}^{-1/2}\mathscr{A}(\nu)\bar{\bar{\sigma}}^{-1/2}$ we construct $\bar{\bar{D}}(\nu)$ and $\bar{\bar{T}}(\nu)$.

Finding $\bar{\bar{\sigma}}^{-1/2}$. We note that for a given diagonal matrix $\bar{\bar{\sigma}} = diag(\sigma_{11}, \sigma_{22}, \sigma_{33})$ with positive elements on the diagonal the matrix $\bar{\bar{\sigma}}^{-1/2}$ is given by $\bar{\bar{\sigma}}^{-1/2} = diag\left(\frac{1}{\sqrt{\sigma_{11}}}, \frac{1}{\sqrt{\sigma_{22}}}, \frac{1}{\sqrt{\sigma_{33}}}\right)$. For the given positive definite non-diagonal matrix $\bar{\bar{\sigma}}$ we construct an orthogonal matrix $\bar{\bar{R}}$ by eigenfunctions of $\bar{\bar{\sigma}}$ such that $\bar{\bar{R}}^T\bar{\bar{\sigma}}\bar{\bar{R}} = \bar{\bar{L}} \equiv diag(\lambda_1, \lambda_2, \lambda_3)$, where $\bar{\bar{R}}^T$ is the transpose matrix to $\bar{\bar{R}}$ and $\lambda_k > 0$, $k = 1,2,3$ are eigenvalues of $\bar{\bar{\sigma}}$. Then $\bar{\bar{\sigma}}^{1/2}$ is defined by $\bar{\bar{\sigma}}^{1/2} = \bar{\bar{R}}\bar{\bar{L}}^{1/2}\bar{\bar{R}}^T$, where $\bar{\bar{L}}^{1/2} = diag(\sqrt{\lambda_1}, \sqrt{\lambda_2}, \sqrt{\lambda_3})$. The matrix $\bar{\bar{\sigma}}^{-1/2}$ is the inverse to $\bar{\bar{\sigma}}^{1/2}$.

Finding $\bar{\bar{D}}(\nu)$ and $\bar{\bar{T}}(\nu)$. Let us take the given positive semi-definite matrix $\mathscr{A}(\nu)$ and the matrix $\bar{\bar{\sigma}}^{-1/2}$ which assumed to be found. Let us consider the matrix $\bar{\bar{\sigma}}^{-1/2}\mathscr{A}(\nu)\bar{\bar{\sigma}}^{-1/2}$ which is symmetric positive semi-definite. The diagonal matrix $\bar{\bar{D}}(\nu)$ is constructed by eigenvalues of $\bar{\bar{\sigma}}^{-1/2}\mathscr{A}(\nu)\bar{\bar{\sigma}}^{-1/2}$. The columns of the orthogonal matrix $\bar{\bar{Q}}(\nu)$ are formed by normalized orthogonal eigenfunctions of $\bar{\bar{\sigma}}^{-1/2}\mathscr{A}(\nu)\bar{\bar{\sigma}}^{-1/2}$ corresponding to eigenvalues $d_k(\nu)$, $k = 1,2,3$. The matrix $\bar{\bar{T}}(\nu)$ is defined by the formula $\bar{\bar{T}}(\nu) = \bar{\bar{\sigma}}^{-1/2}\bar{\bar{Q}}(\nu)$. We note that computing $\bar{\bar{D}}(\nu)$, $\bar{\bar{T}}(\nu)$ and $\bar{\bar{T}}^T(\nu)$ for the reduction of matrices $\mathscr{A}(\nu)$ and $\bar{\bar{\sigma}}$ is similar to the procedure from the paper [Yakhno (2005)].

Step 3: Deriving a solution of (11). Let $\bar{\bar{D}}(\nu)$ and $\bar{\bar{T}}(\nu)$, satisfying (13), be constructed. We find a solution of (11) in the form $\tilde{\mathbf{E}}^k(\nu,t) = \bar{\bar{T}}(\nu)\mathbf{Y}^k(\nu,t)$, where $\mathbf{Y}^k(\nu,t)$ is unknown vector function. Substituting $\tilde{\mathbf{E}}^k(\nu,t) = \bar{\bar{T}}(\nu)\mathbf{Y}^k(\nu,t)$ into (11) and then multiplying the obtained differential equation by $\bar{\bar{T}}^T(\nu)$ and using (13) we find

$$\frac{d\mathbf{Y}^k}{dt}+\frac{1}{\mu_0\sigma_0}\bar{\bar{D}}(\nu)\mathbf{Y}^k=-\frac{1}{\sigma_0}\bar{\bar{T}}^T(\nu)\mathbf{e}^k\delta'(t), \quad \tilde{\mathbf{Y}}^k\Big|_{t<0}=0. \tag{14}$$

Using the ordinary differential equations technique (see, for example [Boyce and DiPrima (1992)]), a solution of the initial value problem (14) is given by

$$\mathbf{Y}^k(\nu,t)=-\frac{1}{\sigma_0}\delta(t)\bar{\bar{T}}^T(\nu)\mathbf{e}^k$$

$$+\theta(t)\frac{1}{\mu_0\sigma_0^2}\bar{\bar{D}}(\nu)\exp\left(-\frac{1}{\mu_0\sigma_0}\bar{\bar{D}}(\nu)t\right)\bar{\bar{T}}^T(\nu)\mathbf{e}^k, \tag{15}$$

where $\nu\in R^3$, $t\in R$; $\theta(t)=1$ for $t\geq 0$ and $\theta(t)=0$ for $t<0$; $\exp\left(-\frac{1}{\mu_0\sigma_0}\bar{\bar{D}}(\nu)t\right)$ is the diagonal matrix whose diagonal elements are $\exp\left(-\frac{d_n(\nu)}{\mu_0\sigma_0}\right)$, $n=1,2,3$.

Step 4: Deriving a solution $\mathbf{E}^k(x,t)$ of (9). The electric field $\mathbf{E}^k(x,t)$ satisfying (9) is found by the inverse Fourier transform $\mathscr{F}_\nu^{-1}$ to the constructed Fourier image of the electric field $\tilde{\mathbf{E}}^k(\nu,t)=\bar{\bar{T}}(\nu)\mathbf{Y}^k(\nu,t)$, $\nu=(\nu_1,\nu_2,\nu_3)\in R^3$, $\quad t\in R$, i.e. the explicit formula for the electric field is given by

$$\mathbf{E}^k(x,t) \quad = \quad \frac{1}{(2\pi)^3}\int_{-\infty}^{+\infty}\int_{-\infty}^{+\infty}\int_{-\infty}^{+\infty}\bar{\bar{T}}(\nu)\mathbf{Y}^k(\nu,t)e^{-i\nu x}d\nu_1 d\nu_2 d\nu_3, \tag{16}$$

where $\mathbf{Y}^k(\nu,t)$ is defined by (14).

4 Deriving the Magnetic Dyadic Green's Function

Step 5: Writing (10) **in terms of the Fourier images with respect to** $x=(x_1,x_2,x_3)\in R^3$. Let $\tilde{\mathbf{H}}^k(\nu,t)$ be the Fourier transform image of the magnetic field $\mathbf{H}^k(x,t)$ with respect to $x=(x_1,x_2,x_3)\in R^3$. Then equations (10) can be written in the form of their Fourier images as follows

$$\frac{\partial\tilde{\mathbf{H}}^k(\nu,t)}{\partial t}=\frac{i}{\mu_0}\left[\nu\times\tilde{\mathbf{E}}^k(\nu,t)\right], \quad \tilde{\mathbf{H}}^k(\nu,t)\Big|_{t<0}=0, \tag{17}$$

where $\nu=(\nu_1,\nu_2,\nu_3)\in R^3$, $t\in R$, $i^2=-1$.

Step 6: Explicit formula for the solution of (17).

A solution of the initial value problem (17) is found by the integration. This solution is given by

$$\tilde{\mathbf{H}}^k(\nu,t) = \theta(t)\frac{i}{\mu_0}\left[\nu \times \int_{-\infty}^{t} \tilde{\mathbf{E}}^k(\nu,\tau)d\tau\right]. \tag{18}$$

Using $\tilde{\mathbf{E}}^k(\nu,t) = \bar{\bar{T}}(\nu)\mathbf{Y}^k(\nu,t)$, the formula (15) and properties of the Dirac delta function we find from (17)

$$\tilde{\mathbf{H}}^k(\nu,t) = -\theta(t)\frac{i}{\mu_0\sigma_0}\left[\nu \times \bar{\bar{T}}(\nu)\bar{\bar{T}}^T(\nu)\mathbf{e}^k\right]$$

$$+\theta(t)\frac{i}{\mu_0^2\sigma_0^2}\left[\nu \times \int_0^t \bar{\bar{T}}(\nu)\exp\left(-\frac{1}{\mu_0}\bar{\bar{D}}(\nu)\tau\right)\bar{\bar{T}}^T(\nu)\mathbf{e}^k d\tau\right]. \tag{19}$$

Step 7: Deriving a solution $\mathbf{H}^k(x,t)$ of (10). The magnetic field $\mathbf{H}^k(x,t)$, satisfying (10), is determined by the inverse Fourier transform $\mathscr{F}_\nu^{-1}$ to the constructed Fourier image of the magnetic field $\tilde{\mathbf{H}}^k(\nu,t)$, $\nu = (\nu_1,\nu_2,\nu_3) \in R^3$, $\quad t \in R$, i.e. the explicit formula for the magnetic field is given by

$$\mathbf{H}^k(x,t) = \frac{1}{(2\pi)^3}\int_{-\infty}^{+\infty}\int_{-\infty}^{+\infty}\int_{-\infty}^{+\infty} \tilde{\mathbf{H}}^k(\nu,t)e^{-i\nu x}d\nu_1 d\nu_2 d\nu_3, \tag{20}$$

where $\tilde{\mathbf{H}}^k(\nu,t)$ is defined by (19).

5 Computational experiments

To demonstrate the robustness of the suggested method for deriving electric and magnetic Green's matrices of the Maxwell's equations in quasi-static approximation we consider a conductive medium which models a geological tissue. The electric dyadic Green's function $\mathscr{G}^E(x-x^0,t-t^0)$ and the magnetic dyadic Green's function $\mathscr{G}^H(x-x^0,t-t^0)$ are defined as 3×3 matrices whose kth columns are electric and magnetic fields $\mathbf{E}^k(x-x^0,t-t^0)$, $\mathbf{H}^k(x-x^0,t-t^0)$, arising from impulsive current dipoles $\mathbf{e}^k\delta(x-x^0)\delta(t-t^0)$, where $k=1,2,3$; $\mathbf{e}^1=(1,0,0)^T$, $\mathbf{e}^2=(0,1,0)^T$, $\mathbf{e}^3=(0,0,1)^T$. For this anisotropic medium we have taken $x^0=0$, $t^0=0$. Applying steps 1–3 and 5, 6 of Sections 3, 4 we have constructed explicit formulae for a non-singular matrix $\bar{\bar{T}}$ and a diagonal matrix $\bar{\bar{D}}(\nu)$ using symbolic computations in MATLAB. Using (15), (19) the explicit formulae for $\tilde{\mathbf{E}}^k(\nu,t)$ and $\tilde{\mathbf{H}}^k(\nu,t)$ have been found explicitly. For the computation of kth column of electric and magnetic dyadic Green's function for equations of electrodynamics in quasi-static approximation we have used the formulae (16), (20). Applying steps 4, 7 of Sections

3, 4 we have computed numerically integrals of (16), (20). For the computation of these integrals we have replaced 3D integration over the whole space R^3 by the integration over the bounded domain $(-A,A)\times(-A,A)\times(-A,A)$ and then approximate 3D integrals over this bounded domain by the following triple integral sums

$$\frac{1}{(2\pi)^3}\sum_{n=-N}^{N}\sum_{m=-N}^{N}\sum_{l=-N}^{N}\left[\bar{\bar{T}}(\nu)\mathbf{Y}^k(\nu,t)\right]_{\nu=(n\Delta\nu,m\Delta\nu,l\Delta\nu)} e^{-i\Delta\nu(nx_1+mx_2+lx_3)}(\Delta\nu)^3,$$

$$\frac{1}{(2\pi)^3}\sum_{n=-N}^{N}\sum_{m=-N}^{N}\sum_{l=-N}^{N}\left[\tilde{\mathbf{H}}^k(\nu,t)\right]_{\nu=(n\Delta\nu,m\Delta\nu,l\Delta\nu)} e^{-i\Delta\nu(nx_1+mx_2+lx_3)}(\Delta\nu)^3.$$

Here N is the natural number for which $A=N\Delta\nu$ and real numbers A and $\Delta\nu$ have been chosen using explicit formulae for columns of the magnetic dyadic Green's function in a homogeneous isotropic conductive space and some empirical observations described below. The homogeneous isotropic conductive space has been taken with characteristics $\mu_0=1.257\times10^{-6}\quad(H\cdot m^{-1})$ and $\sigma_0=10^7\quad(S\cdot m^{-1})$. Using values of $\tilde{\mathbf{H}}^3(\nu,t)$, which have been derived by the formula (19), we have computed values of the second sum mentioned above for different A and $\Delta\nu$. On the other hand we know that the analytical computation of the explicit formulae for the magnetic dyadic Green's function columns of electrodynamics in quasi-static approximation in the isotropic conductive space offers no difficulty (see, for example, [Bowler and Fu (2006)]). For example, the explicit formula of the third column of this magnetic dyadic Green's function is given by

$$\mathbf{H}^3(x,t)=curl_x(\mathbf{e}^3\phi(x,t)),$$

where

$$\phi(x,t)=\frac{\theta(t)}{8}\sqrt{\frac{\mu_0\sigma_0}{\pi^3t^3}}\exp\left(-\frac{\mu_0\sigma_0|x|^2}{4t}\right).$$

Using this formula we have found exact values for the third column $\mathbf{H}^3(x,t)$ of the magnetic dyadic Green's function. The numbers A and $\Delta\nu$ have been chosen such that the difference between values of $\mathbf{H}^3(x,t)$ and values of the third column of the magnetic dyadic Green's function of electrodynamics in quasi-static approximation in the isotropic conductive space obtained by our method becomes negligible. We have chosen $A=60$ and $\Delta\nu=0.5$ as suitable numbers for the computation of our example.

We note that another time scale has been used for the numerical computations of $\mathbf{E}^k(x,t)$ and $\mathbf{H}^k(x,t)$. This time scale is given by $\bar{t}=t/(\mu_0\sigma_0)$ and formulae

(15), (16) and (19), (20) have been written in terms of a new variable $\bar{t}$ and all computations have been made for vector functions $\tilde{\mathbf{E}}^k(\nu,\bar{t}\mu_0\sigma_0)$, $\mathbf{E}^k(x,\bar{t}\mu_0\sigma_0)$ and $\tilde{\mathbf{H}}^k(\nu,\bar{t}\mu_0\sigma_0)$, $\mathbf{H}^k(x,\bar{t}\mu_0\sigma_0)$.

The homogeneous geological tissue is characterized by the magnetic permeability $\mu_0\bar{\bar{I}} \quad (H\cdot m^{-1})$, where $\mu_0 = 1.257\times 10^{-6}$ (see, for example, [Neuman and Alumbaugh (2002)], [Commer et al. (2008)]) and the conductivity tensor $\sigma = \sigma_0\bar{\bar{\sigma}} \quad (S\cdot m^{-1})$,where $\sigma_0 = 10^7$, $\bar{\bar{\sigma}} = diag(9,25,36)$ (see, for example, [Commer et al. (2008)]).

Fig.1(a),1(c),1(e) show 2-D plot of the element $E_1^3(x,t)$ of the dyadic electric function for $x_2 = 0$, $t = 0.1\times 10$, $t = 1\times 10$, $t = 2\times 10$ in seconds. The horizontal axes in Fig.1(a),1(c),1(e) are x_1 and x_3 in meters. Fig.1(b),1(d),1(f) demonstrate 2-D plot of the element $H_1^3(x,t)$ of the dyadic magnetic function for $x_3 = 0$, $t = 0.1\times 10$, $t = 1\times 10$, $t = 2\times 10$. The horizontal axes in Fig.1(b),1(d),1(f) are x_1 and x_2 in meters. In Fig.2(a), 2(b) 2-D and 3-D plots of the same surface $E_1^3(x_1,0,x_3,t)$ ($t = 0.1\times 10$) are presented and Fig.2(c), 2(d) present 2-D and 3-D plots of the surface the $H_1^3(x_1,x_2,0,t)$ ($t = 3\times 10$). Fig.2(b), 2(d) are the view of the surfaces $E_1^3(x_1,0,x_3,t)$ and $H_1^3(x_1,x_2,0,t)$ ($t = 3\times 10$) from the axis z, i.e. from the top.

We note that for an arbitrary fixed t the behavior of the surfaces generated by $H_1^3(x_1,x_2,0,t)$ is similar to the behavior of the surfaces of the function $x_2\exp(-\mu_0\sigma_0(x_1^2+x_2^2)/(4t))$ and the surfaces obtained by $E_1^3(x_1,0,x_3,t)$ are similar to the surfaces of the function $x_1x_3\exp[-\mu_0\sigma_0(x_1^2+x_3^2)/(4t)]$ both deformed by 'astigmatism' of the considered anisotropy.

The elements of dyadic electric and magnetic functions, which exhibit the characteristics of a pulse dipole with the fixed polarization, are initially localized and rising a maximum while spreading laterally and eventually relaxing toward zero. The dynamic variation of electric and magnetic fields (electromagnetic radiation from the dipole) is presented by simulated images.

6 Conclusion

The explicit formulae of dyadic electric and magnetic Green's functions of the time-dependent Maxwell's system in quasi-static approximation for conductive anisotropic media have been derived by the matrix transformations, solutions of some ordinary differential equations depending on the Fourier parameters and the inverse Fourier transform. The formulae for electric and magnetic dyadic Green's functions have been presented in the form that is convenient for computation of the transient electric and magnetic fields. The computational example has confirmed the robustness of the method.

The dyadic Green's functions can be applied as a useful tool for the Boundary El-

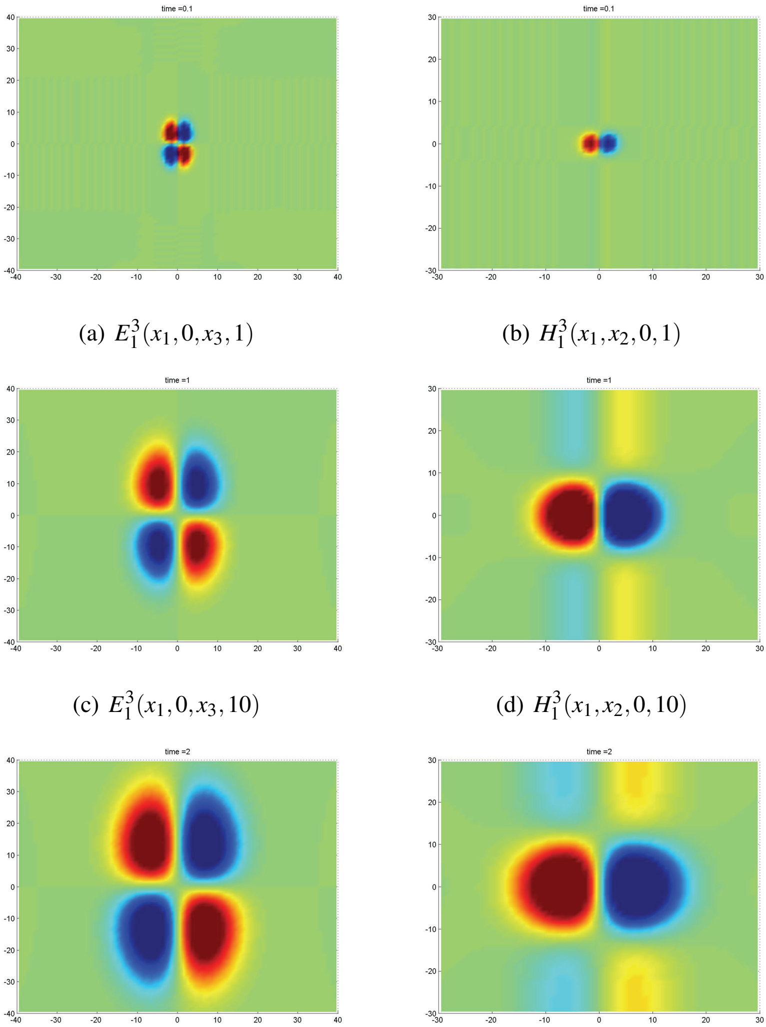

(a) $E_1^3(x_1, 0, x_3, 1)$ (b) $H_1^3(x_1, x_2, 0, 1)$

(c) $E_1^3(x_1, 0, x_3, 10)$ (d) $H_1^3(x_1, x_2, 0, 10)$

(e) $E_1^3(x_1, 0, x_3, 20)$ (f) $H_1^3(x_1, x_2, 0, 20)$

Figure 1: 2-*D* plots of the elements $E_1^3(x_1, 0, x_3, t)$ and $H_1^3(x_1, x_2, 0, t)$ of the electric and magnetic dyadic Green's functions for $t = 0.1 \times 10$, $t = 1 \times 10$, $t = 2 \times 10$ in the anisotropic medium with the conductivity $\sigma = \sigma_0 \bar{\bar{\sigma}} \quad (S \cdot m^{-1})$, $\sigma_0 = 10^7$, $\bar{\bar{\sigma}} = diag(9, 25, 36)$ and the relative magnetic permeability $\mu_0 \bar{\bar{I}} \quad (H \cdot m^{-1})$, $\mu_0 = 1.257 \times 10^{-6}$.

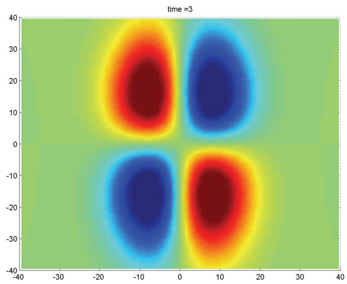

(a) 2-D plot of $E_1^3(x_1,0,x_3,30)$

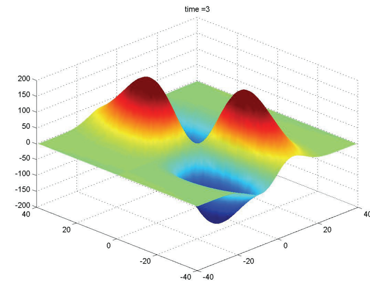

(b) 3-D plot of $E_1^3(x_1,0,x_3,30)$

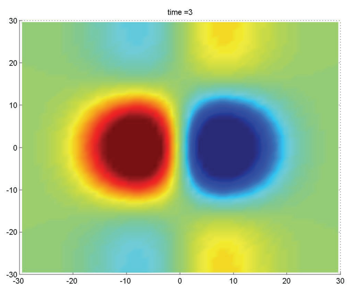

(c) 2-D plot of $H_1^3(x_1,x_2,0,30)$

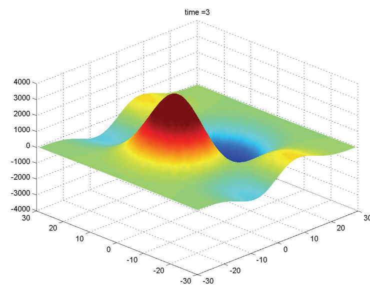

(d) 3-D plot of $H_1^3(x_1,x_2,0,30)$

Figure 2: 2-D and 3-D plots of elements $E_1^3(x_1,0,x_3,30)$ and $H_1^3(x_1,x_2,0,30)$ of the electric and magnetic dyadic Green's functions in the anisotropic medium with the conductivity $\sigma = \sigma_0\bar{\bar{\sigma}} \quad (S \cdot m^{-1})$, $\sigma_0 = 10^7$, $\bar{\bar{\sigma}} = diag(9,25,36)$ and the relative magnetic permeability $\mu_0\bar{\bar{I}} \quad (H \cdot m^{-1})$, $\mu_0 = 1.257 \times 10^{-6}$.

ement Method (BEM). We note that BEM is used for solving problems for partial differential equations in bounded domains with given boundary conditions. In this case the partial differential formulation of the problems is transformed to a boundary integral equations with Green's functions. By discretizing the boundary with finite boundary small patches (boundary elements) the boundary integral equation is reducible to matrix-vector equations. Hence, to apply BEM we need to know the values of Green's functions in a finite number of points (points of discretization). Finding Green's function values at given finite number of points is an important step of BEM. We note that the Green's function values can be easily calculated for a few number of partial differential equations, such as Laplace, Helmholtz, wave, diffusion. Unfortunately Green's function values are not easy to find for many equations and systems. The example of Section 4 in our paper demonstrates the real possibility to compute Green's function values at a finite number of points

(x,t) for the time-dependent Maxwell's equations in quasi-static approximations in anisotropic media. The computation of Green's function values is based on explicit formulae for the Fourier images of dyadic magnetic and electric Green's functions $\tilde{\mathscr{G}}^H(\nu,t)$ and $\tilde{\mathscr{G}}^E(\nu,t)$, respectively, and numerical computation of triple integral at a finite number of points (x,t).

Acknowledgement: This work was supported by Dokuz Eylul University of Turkey under the Research Grant 2006.KB.FEN.024.

References

Bowler, J. R. (1999): Time domain half-spce dyadic Green's functions for eddy-current calculations. *Journal of Applied Physics*, vol.**86**, no.11, pp. 6494–6500.

Bowler, J. R.; Fu, F. (2006): Time-domain dyadic Green's function for an electric source in a conductive plate. *IEEE Transactions on Magnetics*, vol. **42**, no.11, pp. 3661–3668.

Boyce, W. E.; DiPrima, R. C. (1992): *Elementary Differential Equations and Boundary Value Problems*, Wiley, New York.

Chen, J. T.; Ke, J. N.; Liao, H. Z. (2009): Construaction of Green's function using null-field integral approach for Laplace problems with circular boundaries. *CMC: Computers, Materials and Continua*, vol. 9, pp. 93-109.

Chew, W. C. (1990): *Waves and Fields in Inhomogeneous Media*. Van Nostrand Reinhold, New York.

Commer, M.; Neuman, G. A.; Carazzone, J. J. et al. (2008): Massively parallel electrical-conductivity imaging of hydrocarbons using the IBM Blue Gene/L supercomputer. *IBM Journal of Research and Development*, **52**, no. 1/2, pp. 93–103.

Darvas, F.; Pantazis, D.; Kucukaltun-Yildirim, E. (2004): Mapping human brain function with MEG and EEG: methods and validation. *NeuroImage*, vol. **23**, pp. 289–299.

Dirks, H. K. (1996): Quasi-stationary fields for microelectronic Applications. *Elecrical Enfineering* , vol. **79**, pp. 145–155.

Goldberg, J. L. (1992): *Matrix Theory with Application*. Mc-Graw-Hill, New York.

Gu, M. H.; Young, D. L.; Fan, C. M. (2009): the method of fundamental solutions for one-dimensional wave eqautions. *CMC: Computers, Materials and Continua*, vol. 11, pp. 185-208.

Hong, Y. P.; Horn, R. A.; Johnson, C. R. (1986): On the reduction of pairs of Hermitian or symmetric matrices to diagonal form by congruence. *Linear Algebra Appl.*, vol. **73**, pp. 213–226.

Kong, J. A. (1986): *Electromagnetic Wave Theory*. Tech John Wiley and Sons, New York.

Lindell, I. V.; Sihvola, A. H.; Tretyakov, S. A.; Vitanen, A. J. (2002): *Electromagnetic Waves in Chiral and Biisotropic Media*. Artech House, New York.

Nakamura, G.; Tanuma, K. (1997): A formula for the fundamental solution of anisotropic elasticity. *The Quarterly Journal of Mechanics and Applied Mathematics*, vol. 50, pp. 179-194.

Neuman, G. A.; Alumbaugh, D. L. (2002): Three-dimensional induction logging problems, Part 2: A finite-differece solotion. *Geophysics*, vol. **67**, no. 2, pp. 484–491.

Pan, E.; Yuan, F. G. (2000): Three-dimensional Green's functions in anisotropic bimaterials. *International Journal of Solids and Structures*, vol. 37, pp. 5329-5351.

Rashed, Y. F. (2005): Green's first identity method for boundary-only solution of self-weight in BEM formulation for thick slabs. *CMC: Computers, Materials and Continua*, vol. 1, pp. 319-326.

Sekino, M.; Yamaguchi, K. (2003): Conductive tensor imaging of the brain using diffusion-weighted magnetic resonance imaging *Journal of Applied Physics*, vol. **93**, no. 10, pp. 6730–6732.

Tai, C. T. (1994): *Dyadic Green's Functions in Electromagnetic Theory*, IEEE Press, New Jersey.

Tewary, V. K. (1995): Computationally efficient representation for elastodynamic and elastostatic Green's functions for anisotropic solids. *Physical Review B*, vol. 51, pp. 15695–15702.

Tewary, V. K. (2004): Elastostatic Green's function for advanced materials subject to surface loading. *Journal of Engineering Mathematics*, vol. 49, pp. 289–304.

Tewary, V. K.; Bartolo L. M.; Powell A. C. (2002): Green's Functions Experts Meeting and the GREEN Digital Library. NIST Workshop Report. [Online]. *Available: http://www.ctcms.nist.gov/gf/ [April 25, 2002].*

Ting, T. C. T. (2000): Recent developments in anisotropic elasticity. *International Journal of Solids and Structures*, vol. 37, pp. 401-409.

Ting, T. C. T. (2005): Green's Functions for a Bimaterial Consisting of Two Orthotropic Quarter Planes Subjected to an Antiplane Force and a Secrew Dislocation. *Mathematics and Mechanics of Solids*, vol. 10, , no. 2, pp. 197 - 211.

Vagner, D., Lembrikov, B. I.; Wyder, P. (2004): *Electrodynamics of Magnetoactive Media*, Springer, New York, 2004.

Vladimirov, V. S. (1971): *Equations of Mathematical Physics*. Dekker, New York.

Wang, T.; Fang, S. (2001): 3-D electromagnetic anisotropic modeling using finite differences. *Geophysics*, vol. **66**, pp. 1386–1398.

Weiss, C. J.; Newmann, G. A. (2002): Electromagnetic induction in a fully 3D anisotropic earth. *Geophysics*, Vol. **67**, pp. 1104–1114.

Weiss, C. J.; Newmann, G. A. (2003): Electromagnetic induction in a general 3D anisotropic earth, Part 2: The LIN preconditioner. *Geophysics*, vol. **68**, pp. 922–930.

Yakhno, V. G. (2005): Constructing Green's function for the time-dependent Maxwell system in anisotropic dielectrics. *Journal of Physics A: Mathematical and General*, vol. 38, no. 10, pp. 2277–2287.

Yakhno, V. G.; Yakhno, T. M. (2007): Modeling and simulation of electric and magnetic fields in homogeneouis non-dispersive anisotropic materials. *Computers and Structures*, vol. 85, pp. 1623-1634.

Yang, B.; Tewary, V. K. (2008): Green's function for multilayered with interfacial membrane and flexural rigidities. *CMC: Computers, Materials and Continua*, vol. 8, pp. 23-31.

Young, D. L.; Chen, C. S.; Wong, T. K. (2005): Solution of Maxwell's equations using the MQ method. *CMC: Computers, Materials and Continua*, vol. 2, pp. 267-276.